International Journal of Design & Nature and Ecodynamics
Vol. 21, No. 10, October, 2026, pp. 3007-3020
Journal homepage: http://iieta.org/journals/ijdne

Performance Evaluation of a Sustainable Solar-Powered Submersible Pump Irrigation for Remote Indonesian Horticulture

Jeni Paresa[1*], Muh. Akbar[1], Jamaludin[2], Muhamad Rusdi[3]

[1] Department of Civil Engineering, Universitas Musamus, Merauke 99611, Indonesia
[2] Department of Agricultural Engineering, Universitas Musamus, Merauke 99611, Indonesia
[3] Department of Electrical Engineering, Universitas Musamus, Merauke 99611, Indonesia

Corresponding Author Email: jeny@unmus.ac.id

Copyright: ©2026 The authors. This article is published by IIETA and is licensed under the CC BY 4.0 license (http://creativecommons.org/licenses/by/4.0/).

https://doi.org/10.18280/ijdne.211013

Received: 16 August 2026
Revised: 17 October 2026
Accepted: 24 October 2026
Available online: 31 October 2026

Keywords:
solar-powered irrigation, submersible pump, sustainable irrigation, sustainable horticulture, irrigation remote areas

ABSTRACT

Horticultural irrigation in remote Indonesia faces challenges due to limited energy infrastructure, underscoring the need for sustainable irrigation systems. This study aimed to evaluate the technical, operational, social, and economic aspects of solar-powered submersible pump irrigation in Indonesia. An experimental method was employed using a photovoltaic (PV) array system, submersible pump, $LiFePO_4$ battery, hybrid inverter, and Variable Frequency Drive (VFD). The evaluation included seven consecutive days of PV energy measurements, pump discharge and specific energy consumption (SEC), irrigation water losses, energy conversion efficiency, farmer responses, and investment analysis. The results show the PV array generated an average of 1,962.11 Wh/day. The preferred operating point was selected at 40 Hz, delivering a pump discharge of 267.83 L/min and an SEC of 63.09 Wh/m³. The calculated combined efficiency of inverter, battery, and VFD was 84.64%. Water losses through surface-irrigation channels reached 61.54%, requiring a water supply of 32.5 m³/day to meet an effective demand of 12.5 m³/day. Among 30 farmers, 86.67% were interested in adopting the technology. With an initial investment of IDR 55,000,000 and annual savings of IDR 11,379,310/years, the payback period was five years. These findings demonstrate the potential feasibility of sustainable irrigation systems in remote areas of the region.

1. INTRODUCTION

The global agricultural sector faces a major challenge in providing enough food for the world's growing population. The Food and Agriculture Organization projects that food demand will increase by 60% by 2050 [1]. Meanwhile, climate change is exacerbating the crisis by reducing irrigation water availability by up to 34% in tropical regions [2]. In Indonesia, agriculture remains the backbone of the national economy, contributing around 12.4% to the Gross Domestic Product (GDP) and employing 29.5% of the national workforce [3]. However, agricultural productivity in remote areas, especially in eastern Indonesia, is still relatively low. Data from the Ministry of Agriculture of Indonesia show that only 35% of agricultural land in Eastern Indonesia has access to adequate irrigation systems [4].

One area that illustrates this situation is Merauke Regency in South Papua Province. As one of the province's largest agricultural producers, Merauke produces around 2,078 tons of vegetables per year [5], but the lack of a reliable, affordable irrigation system severely hampers the productivity and efficiency of horticultural agriculture in the region. Most farmers rely on gasoline-powered pumps, which consume an average of 60 liters of fuel per hectare, costing around USD 253 per planting season. Initial observations show that 78% of farmers report that irrigation costs account for 40% of total production costs, while 62% experience harvest losses due to high costs and price fluctuations [6]. Dependence on unstable, subsidized fuel exacerbates the situation and makes the region's agricultural production system inefficient and unsustainable [7].

In response, transitioning to an energy-efficient, environmentally friendly, and sustainable irrigation system has become urgent [8, 9]. Solar energy is one of the most promising solutions, especially in areas such as Merauke, which has high solar radiation levels of around 4.8–5.3 kWh/m²/day [10, 11]. From an ecological perspective, solar-powered irrigation technology not only reduces dependence on fossil fuels and lowers emissions associated with conventional systems, but also enhances environmental sustainability by significantly reducing operating costs and improving water-supply resilience in the face of climate change [12]. This technology operates quietly because the pump is submerged in water, does not overheat due to the water's stable temperature, and is more durable than surface water pumps, which typically produce noise and are prone to wear and tear from excessive heat. This system provides a more stable, energy-efficient water supply suitable for horticultural land in remote areas with limited or no access to electricity [13, 14].

This study focuses on the efficiency and energy

performance of solar-powered submersible pump irrigation systems. The study analyzes irrigation efficiency by assessing water distribution in horticultural land and testing soil moisture content to determine plant water requirements and the extent of percolation [15]. In addition to irrigation efficiency, the study evaluates the system's energy performance by comparing the volume of water successfully pumped with available daily solar radiation intensity to assess the effectiveness of solar energy conversion in irrigation operations [16]. This study also examines local farmers' potential to adopt the technology using a descriptive approach, considering technical factors, ease of operation, and farmers' perceptions of the benefits and reliability of socially and contextually relevant systems in remote areas.

Most previous studies have focused on surface-water pumps or solar panel-based irrigation systems implemented in developed urban areas, where communities are relatively tech-savvy. In addition, most previous studies tend to ignore the simultaneous integration of social, technical, and economic analyses in remote areas with development gaps compared to urban areas [16-18]. This study addresses the limited availability of comprehensive investigations on solar-powered submersible pump systems for horticultural irrigation in remote areas where communities exhibit low levels of technological adaptation. In response to limitations in previous studies [18, 19], this work presents a modern irrigation system design that integrates renewable energy sources, submersible pump technology, and energy-efficient water distribution mechanisms. This system is examined through an integrated technical, social, and economic analysis, offering an approach that remains relatively uncommon in the systematic application of horticultural practices, particularly in remote regions of eastern Indonesia.

This research aims to develop and evaluate a solar-powered submersible pump irrigation system to improve water efficiency, reduce production costs, and strengthen the resilience of horticultural irrigation systems in remote areas. This research is expected to contribute tangibly to sustainable agricultural technology by increasing farmer productivity while supporting the Sustainable Development Goals agenda on energy transition and adaptation to climate change [20].

This article is structured into four main sections. The Introduction outlines the research background, urgency, and objectives. Section 2 details the study area, irrigation system design, and data collection and analysis procedures. Section 3 presents the key technical, social, and economic findings of the solar-powered submersible pump implementation. Finally, Section 4, the Conclusions, summarizes the main outcomes and provides recommendations for advancing technological applications in other remote agricultural regions.

2. MATERIALS AND METHODS

2.1 Research site and regional potential

This research was conducted in Isano Mbias Village, Tanah Miring District, Merauke Regency, South Papua Province, Indonesia. This location is at 8°19'18.8" S and 140°27'35.1" E and is one of the active horticultural farming areas in eastern Indonesia. Administratively, this area is classified as a remote rural zone and is not yet served by renewable energy infrastructure or modern irrigation systems.

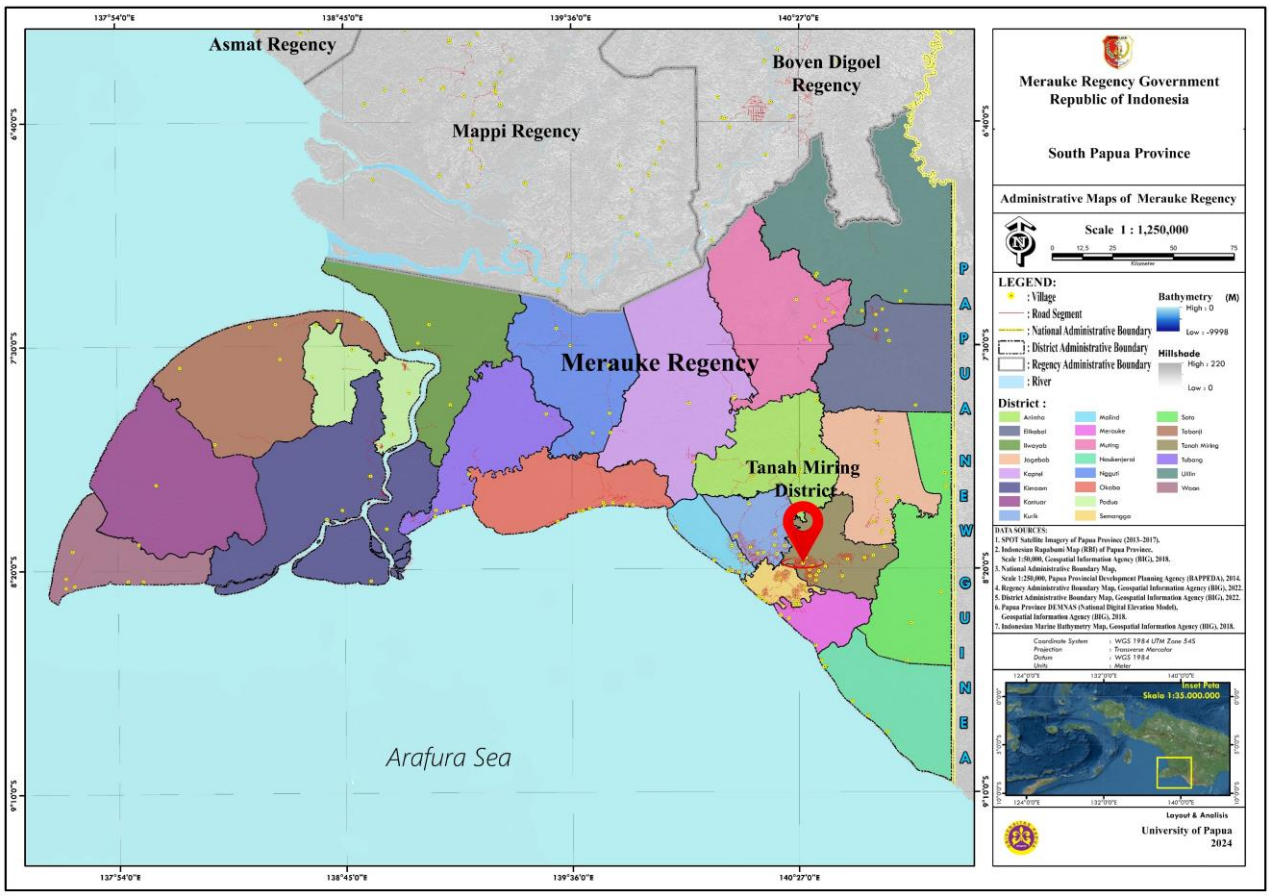

Figure 1. The research was conducted in Isano Mbias Village, Tanah Miring District, Merauke Regency

The test site in Figure 1 is a horticultural garden covering 2,500 m², equivalent to a quarter hectare. The crops cultivated here were annual and seasonal horticultural commodities such as chili peppers, tomatoes, eggplants, and water spinach, which require consistent water availability, especially during the dry season. The land is flat to slightly sloping, with sandy loam soil that infiltrates moderately.

Irrigation water comes from a rainwater reservoir (small reservoir) built next to the garden. This reservoir has a surface area of 37 m², a depth of 2.5 m, and a 1:1.25 slope, with a storage volume of 30.83 m³, providing sufficient capacity to meet irrigation needs during a specific planting period. This reservoir collects water from direct rainfall runoff and is manually refilled from nearby water channels during long dry seasons.

The Tanah Miring region is included in the wet tropical agroclimate zone with two dominant seasons, namely the rainy season between November and April and the dry season between May and October [21]. Average solar radiation in this region reaches 4.8–5.3 kWh/m²/day throughout the year [11], making it an ideal location for solar irrigation technology. Electricity access in this region is limited, with power outages at certain times, making renewable energy a strategic solution to support the sustainability of local agriculture.

This location was selected based on criteria that reflect farmers' need for a cost-effective, environmentally friendly irrigation system that can operate without relying on conventional electricity grids [22]. In addition, this location reflects the general conditions of horticultural land in rural South Papua, which faces similar challenges in access to irrigation and energy. Therefore, this study is not only relevant locally but also has the potential to be replicated more widely in other remote agricultural areas.

This socio-technical assessment focused on horticultural farmers at the study site who represent potential users of the irrigation system. Participants were selected based on their involvement in horticultural farmer groups, their experience with irrigation practices, and their role as user partners in implementing solar-powered irrigation technology. A total of 30 farmers participated in this socio-technical assessment.

2.2 System design

The solar-powered irrigation system designed in this study is an integrated system that aims to meet the water needs of horticultural agriculture in remote areas without access to electricity. The system consists of a main energy source: three 300 Wp photovoltaic (PV) panels connected in parallel, producing a total of 900 Wp. The electrical power from the panels is fed into a 1500 VA Pure Sine Wave Hybrid Inverter, which converts direct current (DC) to alternating current (AC) and is equipped with a 24 V 100 Ah $LiFePO_4$ battery pack with a Battery Management System (BMS). The battery serves as backup energy storage when solar radiation intensity is low [23].

The pumping system uses a Shimge WVSD-75F submersible pump rated at 750 W (1 HP), 220 V, and 50 Hz. This pump is capable of producing a maximum discharge of 21 m³ per hour with a vertical thrust of up to 9 meters and is equipped with an open impeller system. This pump is designed to operate at depths between 0.5 and 5 meters and is made of stainless steel. The pump speed is regulated by a 1.5 kW, 220 V, 1P single-phase AC Variable Frequency Drive (VFD) (2HP Speed-Control Motor Inverter), which controls motor rotation as needed.

The entire system is controlled through a controller box with AC and DC MCBs, motor inverter circuits, on-off switches, and visual indicators. Power consumption and output monitoring are carried out using a Digital Wattmeter and a PZEM-015 DC Wattmeter (up to 200 V and 100 A), which provide real-time data on current, voltage, power, and energy used and stored [24].

2.3 Performance evaluation

This section evaluates the solar-powered submersible pump irrigation system's performance to determine its effectiveness in converting solar energy into mechanical energy for irrigation and its efficiency in distributing water to horticultural land. This evaluation used three main approaches: energy performance evaluation, pump hydraulic evaluation, and assessment of the discharge rate's suitability for irrigation needs.

2.3.1 Solar energy performance analysis

Energy performance evaluation was conducted by measuring the voltage (V), current (A), and power (W) generated by the solar panels throughout the day using a DC wattmeter (PZEM-015) and a digital wattmeter. Field measurements were taken for seven consecutive days, from September 15 to 21, 2025, during the dry season. Data were collected periodically from 6:00 to 17:00 Eastern Indonesian Time (WIT) at UTC+9 to monitor daily variations in PV voltage, current, and power. The period from 09:00 to 14:00 WIT was selected for comparative analysis of PV electrical performance.

PV voltage variations may be influenced by several operating factors, including module temperature, electrical load, and controller operating conditions. Therefore, voltage measurements are interpreted as indicators of PV electrical performance rather than direct measurements of solar irradiance. Daily electrical energy was calculated by integrating power over time (Watt-hours) to determine the total energy available to the system. Additionally, the energy system was evaluated by comparing the PV input power with the pump's actual power consumption.

The total electrical energy generated by the solar panels in a day can be calculated from the average system voltage and the current flowing during the observation period. This energy is expressed in Watt-hours (Wh) and calculated using the following equation:

$$E = V \times Ah \tag{1}$$

where,

E = Generated electrical energy (Wh)

V = Solar panel output voltage (V)

Ah = Total electric charge flowing during a given period (Ah)

Eq. (1) is used to calculate the total electrical energy generated by a PV system in one day, based on the product of the average voltage and the accumulated current flow. E represents the actual energy available for load or storage [25].

2.3.2 Submersible pump performance evaluation

The submersible pump performance was evaluated at operating frequencies of 21, 30, 40, and 50 Hz using a VFD. The measured parameters included flow velocity, pump

discharge, voltage, current, and electrical input and output power. Each operating condition was tested over a one-hour measurement period during peak solar hours, and the test was repeated over seven consecutive days to capture variations in operating conditions.

Pump discharge was determined from the measured flow velocity and the cross-sectional area of the discharge hose. In addition to hydraulic output, the specific energy consumption (SEC) was calculated to quantify the electrical energy required to deliver a unit volume of water. SEC was calculated as:

$$SEC = \frac{P_{in}}{Q} \tag{2}$$

where,

SEC = Specific energy consumption (Wh/m³)

P_{in} = Electrical input power (W)

Q = Pump discharge (m³/h)

The discharge, electrical power, and SEC obtained at each operating frequency were compared to determine the most suitable operating point based on the balance between water delivery capacity and system energy demand. Hydraulic pump efficiency was not directly calculated because hydraulic head or discharge pressure was not measured at each operating frequency. Therefore, the evaluation focused on measured hydraulic output and electrical energy consumption per unit volume of water.

In addition, a lower SEC indicates a lower electrical energy requirement per unit volume of delivered water. However, SEC was interpreted alongside pump discharge because a low SEC alone does not necessarily indicate the most suitable operating condition for field irrigation when the resulting discharge is insufficient to meet the required water demand.

In addition to calculating power, calculations were also made for the cross-sectional area of the cylinder hose (A_p) in Eq. (3) and the pump discharge (Q_p) in Eq. (4) as follows [26, 27]:

$$A_p = \frac{\pi d^2}{4} \tag{3}$$

where,

A_p = Cross-sectional area of a hose (m²)

d = Inner diameter of a hose (m)

$$Q_p = A_p \times v \tag{4}$$

where,

Q_p = Pump water flow rate (m³/s), converted using: Q_p (L/min) = 60,000 × Q_p (m³/s)

v = Water flow velocity (m/s)

2.3.3 Field irrigation flow test and water demand estimation

To assess whether the pump's irrigation discharge meets irrigation water requirements, a flow simulation was conducted in a 1-meter-long surface irrigation channel. The trapezoidal channel was filled with water pumped at the optimal operating frequency. The actual irrigation discharge (Q) was calculated from the filling time (v) and channel volume (A) using Eqs. (5)–(7) [28, 29].

$$A = \frac{b + B}{2} h \tag{5}$$

where,

b = Bottom width = 40 cm = 0.40 m

B = Top width = 85 cm = 0.85 m

h = Water depth = 40 cm = 0.40 m

$$V = A\ell \tag{6}$$

$$Q_{\text{fill}} = \frac{V}{t} = \frac{A\ell}{t} \tag{7}$$

where,

V = Volume of water required to fill the channel (m³)

A = Cross-sectional area of the channel (m²)

$A\ell$ = Length of the channel (m)

Q_{fill} = Average channel filling flow rate (m³/s)

t = Measured filling time (s)

In addition, water loss during irrigation channel conveyance was estimated using a water balance approach, considering the incoming water volume, outgoing water volume, and change in water storage, as expressed in Eq. (8) [30]:

$$V_{\text{loss}} = V_{\text{in}} - V_{\text{out}} - \Delta V_{\text{storage}} \tag{8}$$

where,

V_{loss} = Estimated water loss (m³)

V_{in} = total incoming water volume (m³)

V_{out} = Total outgoing water volume (m³)

$\Delta V_{\text{storage}}$ = Change in water stored within the channel (m³)

To determine the percentage of water loss relative to the total water flow, Eq. (9) is used [30]:

$$Loss(\%) = 100 \times \frac{V_{\text{loss}}}{V_{\text{in}}} \tag{9}$$

This data is used to calculate the total irrigation requirement (Q_{total}) by considering water loss and crop requirements (Q_{plant}). The irrigation water requirement can be calculated using Eqs. (10) and (11) below [29, 31]:

$$Q_{plant} = L_l \times A_g \tag{10}$$

$$Q_{total} = \frac{Q_{plant}}{1 - Loss} \tag{11}$$

where,

Q_{plant} = Daily water requirement for plants (L/day)

Q_{total} = Total volume of water that must be supplied by the system (L/day)

L_l = Irrigated land area (m²)

A_g = Plant water requirement (liters/m²/day), using 5 mm/day = 5 liters/m²/day based on the agronomic value of horticultural water requirements

Loss = Percentage of water loss in the distribution system (decimal)

The operational duration of the pump system (t) is also calculated based on the ratio between the total irrigation requirement (Q_{total}) and the actual pump discharge (q) in Eq. (12) [32].

$$t = \frac{Q_{total}}{q} \tag{12}$$

where,

t = Pump operating time (minutes or hours)

q = Pump flow rate (liters/minute)

2.3.4 Socio-technical feasibility assessment

A socio-technical feasibility assessment was conducted to evaluate the extent to which solar-powered submersible pump irrigation systems can be operated and accepted by farmers in remote areas [33]. The assessment was conducted to evaluate farmers' perceptions, operational experiences, maintenance capabilities, and their willingness to adopt a solar-powered submersible pump irrigation system. This assessment involved 30 horticultural farmers from the study area who represented potential users of this irrigation technology. Participants were selected using purposive sampling based on their active involvement in horticultural farming and their status as potential users of the irrigation system being tested. Data were collected through semi-structured interviews and direct field observations conducted during the system trial. Each interview lasted 15 minutes and was organized around three main themes: (1) ease of system operation and understanding of the pump and control panel; (2) technical and non-technical challenges encountered during operation and maintenance; and (3) willingness to adopt technology for future irrigation activities. The study also made direct observations based on farmers' interactions with the pump, control panel, and irrigation components during system operation. Interview responses were analyzed using descriptive frequency analysis and thematic analysis.

The thematic analysis process was conducted in four stages: (1) Reviewing the responses by identifying statements related to the acceptance, operation, and maintenance of the system; (2) Assigning ordinal codes to relevant statements, such as "willing to adopt the technology," "willing under certain conditions," "unwilling," and "undecided"; (3) Grouping the codes by combining similar codes into the categories "willing to adopt" and "unwilling to adopt"; and (4) Counting the number of respondents in each category and converting the numbers into percentages. For structured responses, the percentage of respondents who selected a particular answer (P) was calculated using the formula:

$$P = \left(\frac{n}{N}\right) \times 100\% \quad (13)$$

where,

n = Number of respondents

N = The total number of participants

3. RESULTS AND DISCUSSION

3.1 System performance

3.1.1 Solar energy performance analysis

Daily variations in PV voltage were monitored between 06:00 and 17:00 WIT over seven consecutive days to evaluate the electrical performance of the PV system.

The PV voltage evaluation for Day 1, shown in Figure 2, indicates that the voltage increased from 24.00 V at 6:00 WIT to 37.93 V at 11:00 WIT. Subsequently, voltage fluctuated due to partial cloud cover, but it remained relatively stable above 33 V until 14:00 WIT. Later, voltage spiked temporarily at 15:00 WIT to 35.34 V, then gradually declined to 22.92 V by 17:00 WIT. The average daily voltage on Day 1 was 31.40 V. This pattern indicates that the PV voltage remained relatively stable during the selected observation period from 09:00 to 14:00 WIT.

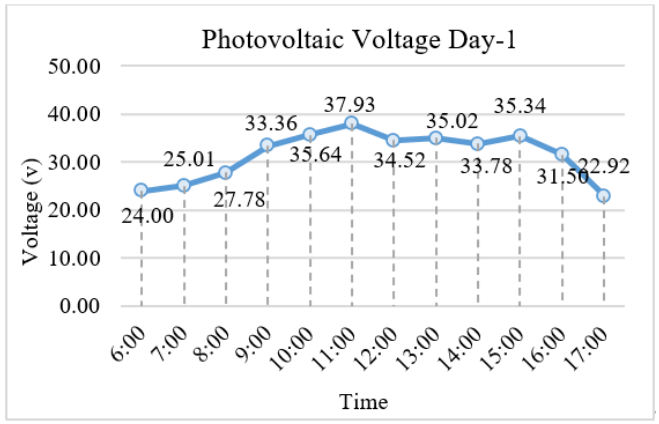

Figure 2. Daily photovoltaic (PV) voltage

The following evaluation presents the PV voltage performance during peak solar radiation intensity from 9:00 WIT to 14:00 WIT over seven consecutive measurement days. The figure compares the voltage response across the observation days to illustrate the variability in PV performance influenced by sunlight availability or weather conditions.

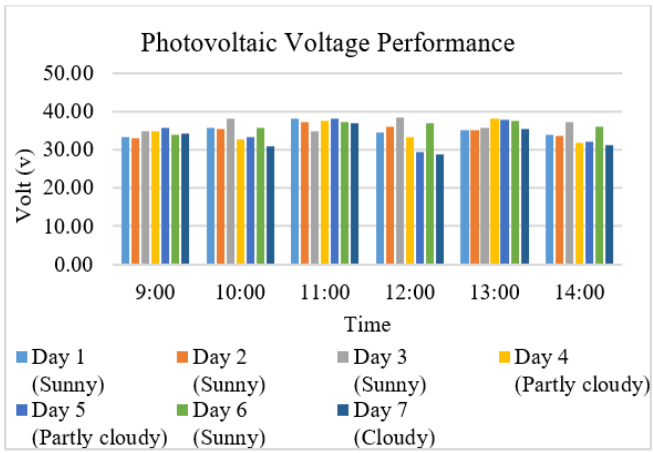

Figure 3. Photovoltaic (PV) voltage over seven days

The seven-day evaluation presented in Figure 3 shows that the PV voltage during the selected observation period from 09:00 to 14:00 WIT ranged from 28.60 to 38.40 V, with an overall mean of 34.91 V. Sunny conditions on Days 1, 2, 3, and 6 produced relatively higher voltage levels, with an average of 35.64 V. In contrast, partly cloudy conditions on Days 4 and 5 resulted in a lower average of 34.49 V. The lowest average voltage occurred on cloudy Day 7 at 32.85 V, with the lowest hourly value of 28.60 V at 12:00 WIT. Despite these fluctuations, the PV voltage generally remained above 30 V during most of the peak period, indicating adequate and relatively stable voltage generation. The observed voltage variations under different weather conditions indicate differences in PV electrical performance during field operation.

After analyzing the voltage, the solar panel's current characteristics were observed to understand how much electricity was available to power the system load.

Figure 4 shows that the PV current increased from 4.42 A at 06:00 WIT to 7.67 A at 11:00 WIT, then gradually declined

in the afternoon. During the peak solar radiation period from 09:00 to 14:00 WIT, the current remained relatively stable, ranging from 6.98 to 7.67 A, with an average of 7.35 A. These variations indicate stable current generation under the observed sunny conditions. After 14:00 WIT, the current decreased from 6.98 A to 2.98 A at 17:00 WIT, indicating a decline in PV output as sunlight availability decreased. Meanwhile, the cumulative PV-side charge output increased continuously throughout the observation period, reaching 66.00 Ah by 17:00 WIT stored in the 24 V/100 Ah $LiFePO_4$ battery.

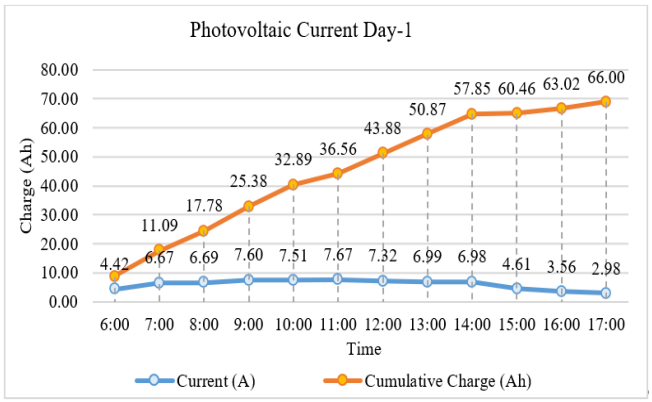

Figure 4. Daily photovoltaic (PV) current

Figure 5 shows the PV current performance during the selected observation period from 09:00 to 14:00 WIT over seven consecutive days of observation. The figure compares the hourly current generated by the PV system under different weather conditions, based on field measurements.

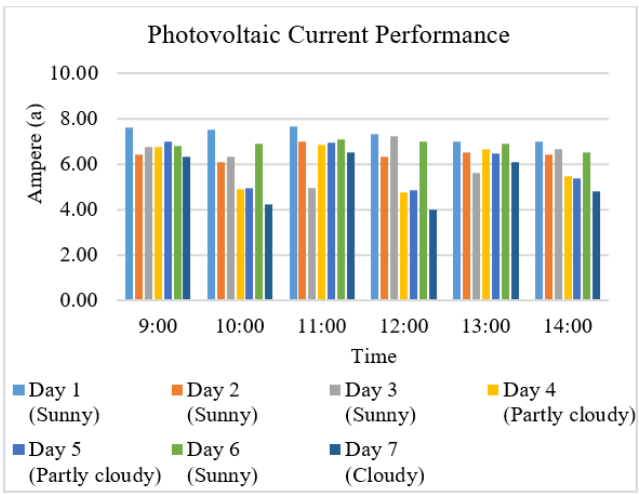

Figure 5. Photovoltaic (PV) current over seven days

Figure 5 shows the PV current performance during the selected observation period from 09:00 to 14:00 WIT, ranging from 4.00 to 7.67 A, with an overall average of 6.29 A. Sunny conditions on Days 1, 2, 3, and 6 produced a higher average current of 6.73 A, compared with 5.91 A under partly cloudy conditions on Days 4 and 5 and 5.32 A under cloudy conditions on Day 7. The highest current of 7.67 A was recorded on Day 1 at 11:00 WIT, while the lowest value of 4.00 A occurred on cloudy Day 7 at 12:00 WIT. Hourly fluctuations occurred across the seven days, particularly at 10:00 and 12:00 WIT, indicating short-term variations in solar availability due to changing weather conditions. Despite these fluctuations, all recorded current values during the selected period were at or above 4.00 A, indicating relatively stable PV current output under the observed field conditions.

The cumulative electrical output generated by the PV system over seven consecutive days of observation. This comparison was conducted to evaluate the consistency of electrical output under varying weather conditions during the field observation period.

The cumulative charge in Figure 6 shows that the PV system ranged from 52.10 to 66.00 Ah/day, with an average of 60.45 Ah/day. The highest cumulative charge was recorded on Day 1 under sunny conditions at 66.00 Ah, followed by Day 6 at 64.60 Ah, while the lowest value occurred on Day 7 under cloudy conditions at 52.10 Ah. The average cumulative charge under sunny conditions was 63.21 Ah/day, compared to 59.10 Ah/day under partly cloudy conditions and 52.10 Ah/day under cloudy conditions. Lower charge generation under cloudy conditions indicates that reduced sunlight availability directly affects the PV system's electrical output. Additionally, the system generated more than 59 Ah/day on six of the seven observation days, indicating relatively consistent charge generation under the observed field conditions.

Variations in PV voltage and current directly affect the PV system's power output and total energy generation. Therefore, the power performance was further evaluated to examine how these electrical parameters contribute to the energy available to the irrigation system. Figure 7 also shows the daily PV power profile on Day 1, including hourly power output and cumulative energy production throughout the day.

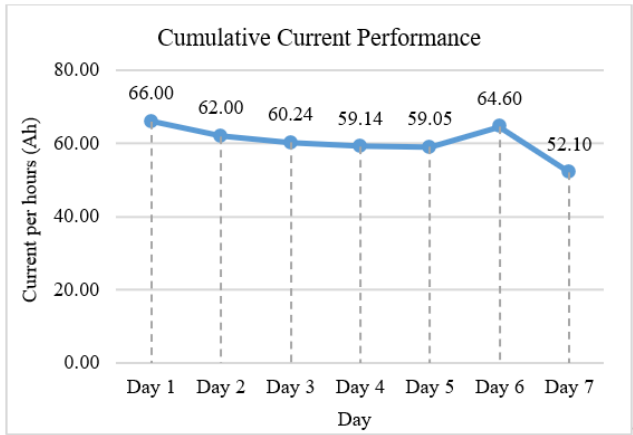

Figure 6. Cumulative charge output

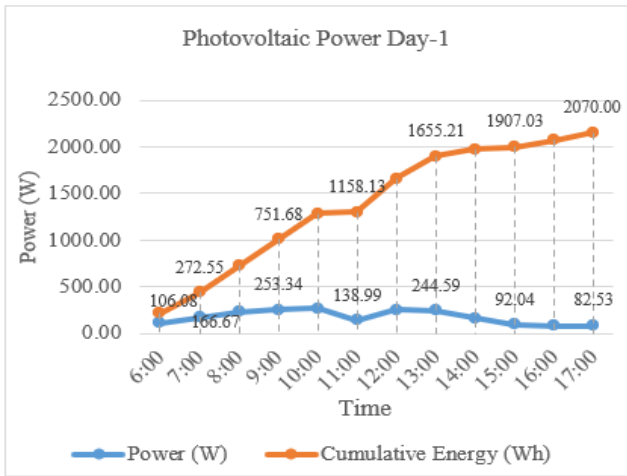

Figure 7. Daily photovoltaic (PV) power

The PV power output shown in Figure 7 illustrates energy production on Day 1 under sunny conditions. PV power increased from 106.08 W at 06:00 WIT to 267.46 W at 10:00 WIT, then fluctuated during the selected daytime observation period. Power output decreased to 138.99 W at 11:00 WIT and rose again to 252.49 W at 12:00 WIT before gradually declining to 82.53 W at 17:00 WIT. These fluctuations reflect variations in the electrical power output of the PV system throughout the day. Conversely, cumulative energy continued to increase, reaching 2,070.00 Wh at 17:00 WIT, indicating that the PV system continued to generate energy throughout the observation period.

The cumulative energy output on Day 1 was estimated using Eq. (1) by multiplying the mean PV voltage of 31.40 V by the cumulative PV-side charge output of 66.00 Ah.

$$E = 31.40\ V \times 66.00\ Ah = 2{,}072.40\ Wh$$

This calculation is highly consistent with the daily energy measurement data of 2,070.00 Wh, indicating that the PV system is operating optimally in absorbing solar energy. The difference between the calculated result of 2,072.40 Wh and the measured result of 2,070.00 Wh is technically acceptable. This discrepancy arises from the rounding of average voltage and current values when recording data fluctuations. The 2.40 Wh (0.12%) difference remains within the system's tolerance limits and does not affect the validity of the results.

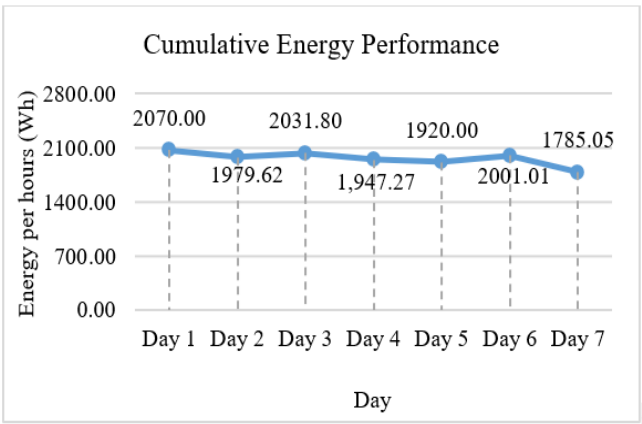

Figure 8. Photovoltaic (PV) power over seven days

Figure 8 expands the analysis by comparing cumulative daily PV energy output over seven consecutive days. Energy generation ranged from 1,785.05 to 2,070.00 Wh/day, with an average of 1,962.11 Wh/day. The highest energy production was recorded on Day 1 under sunny conditions, while the lowest occurred on Day 7 under cloudy conditions. Average energy production was 2,020.61 Wh/day on sunny days, 1,933.64 Wh/day on partly cloudy days, and 1,785.05 Wh/day on cloudy days. This pattern indicates that cloud cover reduces daily energy production, with a 13.8% difference between the highest and lowest values. Despite this variation, the PV system maintained energy production above 1,785 Wh/day throughout the seven-day observation period.

Beyond its technical implications, this energy system supports environmental sustainability by reducing greenhouse gas emissions, fossil fuel consumption, and air pollutants from conventional irrigation systems in remote agricultural areas where energy infrastructure remains limited.

3.1.2 System-level energy balance and loss analysis

To more realistically assess the solar-powered irrigation system's energy performance, the system-level energy balance was evaluated by accounting for losses from inverter conversion, battery charge–discharge cycling, and VFD operation.

The inverter performance was evaluated over seven consecutive days under varying weather conditions by comparing the DC input power with the corresponding AC output power. As presented in Figure 9, the inverter efficiency ranged from 90.43% to 91.64%. On Day 1 under sunny conditions, the DC input power was 1,321.21 W, resulting in an AC output power of 1,210.76 W and an inverter conversion loss of 110.45 W, corresponding to an efficiency of 91.64%. In contrast, on Day 7 under cloudy conditions, the DC input power decreased to 918.66 W, producing an AC output power of 830.74 W. The inverter efficiency was 90.43%, with a conversion loss of 87.92 W.

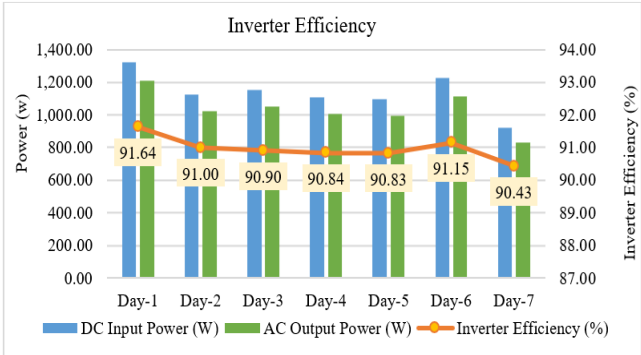

Figure 9. Inverter efficiency

Across the seven-day observation period, the average DC input power was 1,134.74 W, while the average AC output power was 1,032.27 W. The average inverter efficiency was 90.97%, corresponding to an average conversion loss of 102.47 W, or 9.03% of the DC input power. These results indicate that the inverter maintained relatively stable conversion efficiency under the observed weather conditions, although its absolute input and output power varied across the measurement period. The lower input power recorded on Day 7 under cloudy conditions was accompanied by a slightly lower conversion efficiency than that recorded on Day 1 under sunny conditions. The inverter performance over the seven-day observation period is illustrated in Figure 9.

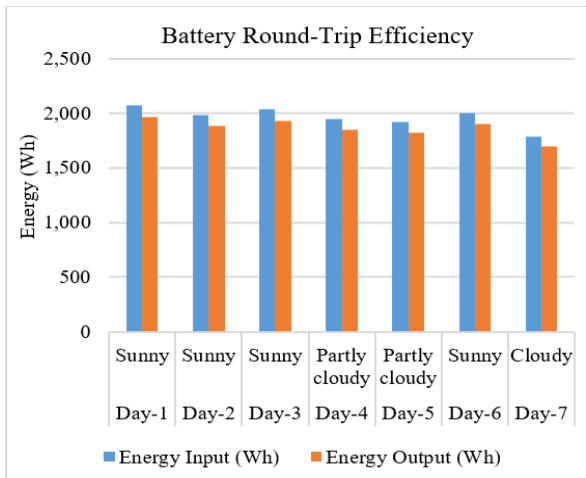

Figure 10. Battery Round-Trip Efficiency (RTE)

Battery storage adds energy losses during charging and discharging. Figure 10 shows the battery charging and discharging process.

Figure 10 illustrates a 24 V, 100 Ah $LiFePO_4$ battery system used as an energy storage unit to support the pump load when PV generation is insufficient. Based on a seven-day energy assessment, the PV energy supplied to the storage system ranged from 1,785.05 to 2,070.00 Wh/day, with an average of 1,962.11 Wh/day. The corresponding daily discharge energy ranged from 1,695.80 to 1,966.50 Wh/day, with an average of 1,864.00 Wh/day. Therefore, the battery's energy efficiency ($\eta_{battery}$) was 95.00%, indicating that 5.00% of the energy supplied to the battery was lost during combined charging and discharging.

The internal conversion efficiency of the VFD was evaluated using one-hour power measurements conducted during the peak solar period over seven consecutive days under varying weather conditions. As shown in Figure 11, average VFD efficiency decreased as operating frequency increased, from 98.20% at 21 Hz to 98.08% at 30 Hz, 97.94% at 40 Hz, and 95.85% at 50 Hz. The corresponding average input and output powers were 174.97 W and 171.83 W at 21 Hz; 601.53 W and 589.96 W at 30 Hz; 1,032.65 W and 1,011.36 W at 40 Hz; and 1,143.09 W and 1,095.65 W at 50 Hz. The largest efficiency drop occurred at 50 Hz under cloudy conditions on Day 7, when VFD efficiency fell to 89.91%. The corresponding input and output powers were 919.59 W and 826.82 W, respectively, resulting in a power conversion loss of 92.77 W. This was substantially higher than the losses observed at lower operating frequencies, as illustrated in Figure 11.

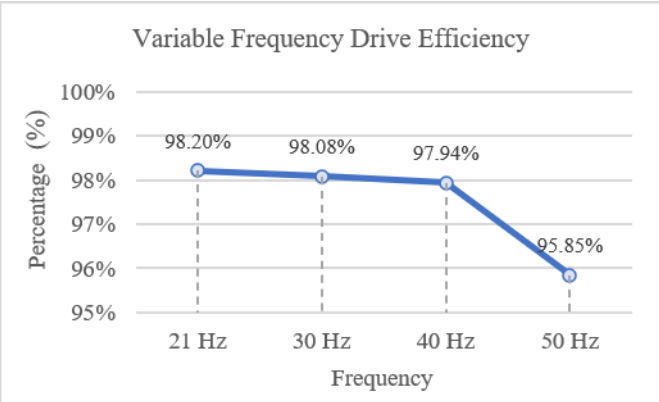

Figure 11. Variable Frequency Drive (VFD) efficiency

Based on the measured performance of the major energy conversion and storage components, the overall system-level efficiency was determined by considering the sequential energy pathway through the inverter, battery, and VFD. The average inverter efficiency was 90.97%, the battery Round-Trip Efficiency (RTE) was 95.00%, and the VFD efficiency at the selected 40 Hz operating point was 97.94%. Accordingly, the combined system-level efficiency was calculated as:

$$\eta_{system} = \eta_{inverter} \times \eta_{battery} \times \eta_{VFD}$$
$$= 0.9097 \times 0.9500 \times 0.9794 = 0.8464 = 84.64\%$$

$$Loss_{system} = 100\% - 84.64\% = 15.36\%$$

Thus, the system-level efficiency reached 84.64%, indicating cumulative conversion and storage losses of 15.36%. Of the average PV energy generation of 1,962.11 Wh/day, only 1,660.73 Wh/day is theoretically available at the VFD output. In comparison, 301.38 Wh/day is lost due to inverter conversion, battery charge–discharge cycles, and VFD power conversion. These results provide a systematic overview of the amount of energy available for irrigation pumps.

The evaluation period in this study was short-term, lasting seven consecutive days. Although these measurements reflect the PV system's daily performance under dry-season weather conditions, the results do not fully represent variations in solar energy production throughout the season or year. Therefore, long-term monitoring across different seasons is recommended to obtain a more comprehensive assessment of the PV system's performance.

3.1.3 Submersible pump performance evaluation

The submersible pump performance was evaluated at four VFD operating frequencies: 21, 30, 40, and 50 Hz. An initial test at 20 Hz showed the pump could not initiate water circulation under the tested conditions because the available motor torque was insufficient to overcome the initial operating load. The pump therefore operated successfully at a minimum frequency of 21 Hz. At this frequency, the pump produced a low discharge of 18.31 L/min, with an average VFD input power of 174.97 W and output power of 171.83 W. The corresponding calculated motor current was 0.78 A. This discharge was considered insufficient for the irrigation requirements of the cultivated area.

Increasing the operating frequency to 30 Hz substantially increased the discharge to 153.57 L/min, with an average VFD input power of 601.53 W and output power of 589.96 W. At 40 Hz, the discharge increased further to 267.83 L/min, while the corresponding VFD input and output powers reached 1,032.65 W and 1,011.36 W, respectively. The calculated motor current at this operating point was 4.60 A, based on the 220 V reference voltage. The 40 Hz discharge was close to the field irrigation flow rate of 270.00 L/min, making this frequency suitable for the tested irrigation application.

At 50 Hz, the pump discharge increased to 350.86 L/min, with an average VFD input power of 1,143.09 W and output power of 1,095.65 W. Although this frequency produced the highest discharge, the inverter reportedly triggered an overload alarm during testing. Consequently, the irrigation system did not operate at 50 Hz because the observed overload indicated a potential limitation in the installed power-conversion system's ability to support this operating condition reliably. To compare the energy required to deliver water at each frequency, the SEC was calculated using the VFD output power supplied to the motor and the measured pump discharge. SEC was calculated as the ratio of electrical power (W) to water discharge (m^3/h), yielding a value in Wh/m^3.

The SEC values presented in Table 1 were 156.84 Wh/m^3 at 21 Hz, 64.19 Wh/m^3 at 30 Hz, 63.09 Wh/m^3 at 40 Hz, and 52.17 Wh/m^3 at 50 Hz. The lowest SEC value was obtained at 50 Hz, indicating the lowest electrical energy requirement per unit volume of water based on the measured power and flow rate. However, this frequency was not selected because the inverter triggered an overload alarm, indicating an operational limitation. Based on these results, 40 Hz at 1,011.36 W was selected as the preferred operating point because it yielded the second-lowest SEC value and a flow rate of 267.83 L/min, significantly higher than the 153.57 L/min at 30 Hz, without triggering the overload alarm observed at 50 Hz.

Table 1. Specific energy consumption (SEC) at different Variable Frequency Drive (VFD) operating frequencies

Freq. (Hz)	Discharge (Q_p) (L/min)	Discharge (m³/h)	VFD P_{in} (W)	VFD P_{out} (W)	SEC (Wh/m³)
21	18.26	1.0956	174.97	171.83	156.84
30	153.19	9.1914	601.53	589.96	64.19
40	**267.17**	**16.0302**	**1032.65**	**1011.36**	**63.09**
50	350	21.0000	1143.09	1095.65	52.17

This system is powered by a 24 V, 100 Ah $LiFePO_4$ battery with 95% RTE, for a total of 2,280 Wh. To further examine the relationship between battery energy availability and pump power requirements, the State of Charge (SOC) was measured during a 120-minute operating period at 10-minute intervals at various VFD operating frequencies (21, 30, 40, and 50 Hz). The following graphs show the overall VFD operating frequencies and the preferred operating point at 40 Hz.

Figures 12 and 13 show battery discharge conditions at various VFD operating frequencies and the relationship between voltage and SOC at 40 Hz. The higher the operating frequency, the faster the SOC decreases. After 120 minutes, the remaining SOC was 82.35%, 39.24%, and 11.28% at 21, 30, and 40 Hz, respectively; at 50 Hz, the SOC reached 4.76% after 100 minutes and 0% after 110 minutes. At 40 Hz, the battery voltage remained stable and gradually decreased due to the pump's power requirements and battery energy consumption, leaving only 11.28% SOC after 120 minutes. At this frequency, the battery voltage decreased from 29.20 V at 100% SOC to 24.26 V at 11.28% SOC.

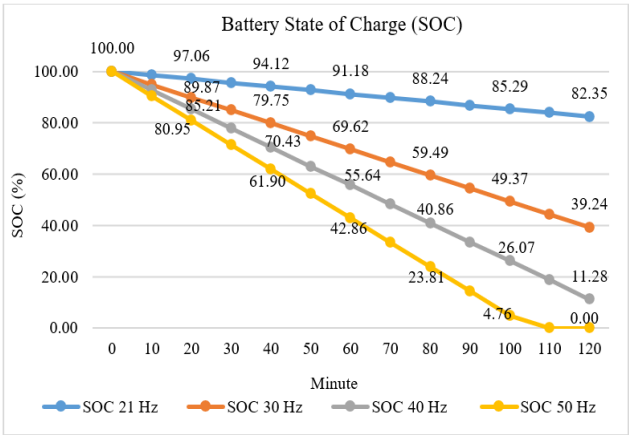

Figure 12. Comparison of State of Charge (SOC) at different Variable Frequency Drive (VFD) operating frequencies

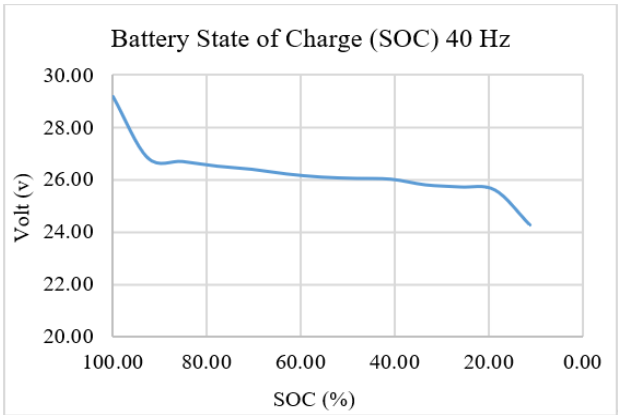

Figure 13. Battery voltage as a function of State of Charge (SOC) at 40 Hz Variable Frequency Drive (VFD) operation

The SOC profiles also show how the battery supports pump operation at different VFD frequencies, particularly at the preferred operating point of 40 Hz. These findings highlight the importance of considering battery energy availability when evaluating pump operating conditions. The battery serves as the primary energy storage component, supplying electricity to the pump through the inverter and VFD when PV generation is insufficient to meet the system's power demand, thereby supporting pump operation subject to the available battery SOC. The pump discharge flow rate and the VFD operating frequency are shown in Figure 14.

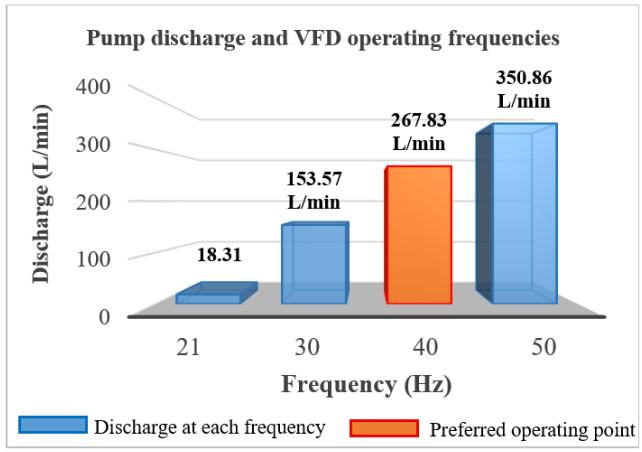

Figure 14. Pump discharge and Variable Frequency Drive (VFD) operating frequencies

In addition, the power of the submersible pump was also analyzed using Eq. (2) at a frequency of 40 Hz, with a voltage of 220 V and an average pump current of 4.6 A:

$$P = 220\ V \times 4.6\ A = 1{,}012\ W$$

The calculated pump power of 1,012 W matches the actual power consumption measured at the VFD output (1,011.36 W at 40 Hz), with a difference of 0.64 W. This difference, less than 0.1%, remains within the tolerance limits for measurement and rounding.

We then measured flow rate and velocity to demonstrate the relationship between frequency and the submersible pump's flow output, as shown in Table 2.

Table 2. Variable Frequency Drive (VFD) measurements based on pump flow rate and water flow velocity

Frequency (Hz)	Hose Diameter (cm)	Flow Cross-Sectional Area (cm²)	Flow Velocity (v) (m/min)	Discharge (Q_p) (L/min)
21	3.18	7.94	23.06	18.31
30	3.18	7.94	193.41	153.57
40	3.18	7.94	337.32	267.83
50	3.18	7.94	441.89	350.86

The pump discharge (Q_p) at each frequency variation is calculated using Eq. (3). In contrast, the flow cross-sectional area (A_p) is calculated using Eq. (4) for a circular cross-section with a hose diameter of 3.18 cm.

Given the value of:

$$d = 3.18 \text{ cm} = 0.0318 \text{ m}$$

$$A_p = \frac{3.1416 \times (0.0318)^2}{4} = \frac{0.003176}{4} = 0.000794\, m^2$$

Using a hose diameter of 3.18 cm, the calculated cross-sectional area is 7.94 cm². This value is consistent with the cross-sectional area reported in Table 2.

This shows the consistency of the measurements and the accuracy of the tool's dimension recording. At 40 Hz, the flow velocity was recorded at 337.32 m/minute. Therefore, the pump discharge (Q_p) can be calculated as follows:

$$Q_p = 0.000794 \times 337.32 = 0.2678\, m^3/\text{minute} = 267.83\, L/\text{minute}$$

Using a hose cross-sectional area of 7.94 cm² and a measured flow velocity of 337.32 m/min, the calculated pump discharge at 40 Hz is 267.83 L/min. This result demonstrates an increase in pump discharge with increasing VFD operating frequency over the tested range.

A technical limitation in measuring this submersible pump's performance is that we did not measure water pressure, or hydraulic head, during pump testing. Therefore, the pump's hydraulic efficiency could not be calculated. This study evaluated pump performance based on flow rate, electrical power, and SEC. Future studies need pressure or hydraulic head measurements to calculate hydraulic efficiency and provide a more comprehensive evaluation of pump performance.

3.1.4 Field irrigation flow test and water demand estimation

Irrigation flow rates are measured directly in the field using a test channel filling method with water from a submersible pump. Measurements are taken by recording the time required to fill a specific channel volume and noting the water flow velocity and channel cross-sectional dimensions. The following is a cross-sectional image of a surface irrigation channel:

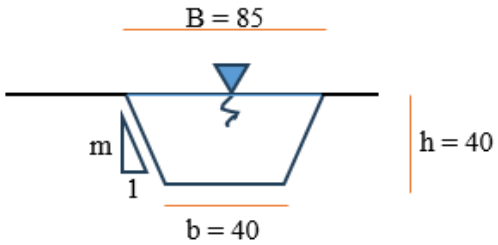

Figure 15. Cross-section of surface irrigation

Based on Figure 15, the channel is trapezoidal in shape with dimensions of bottom width (b) = 40 cm = 0.40 m, top width (B) = 85 cm = 0.85 m, water height (h) = 40 cm = 0.40 m, and side slope = 1:1, which means the horizontal sloping side length = vertical length = 0.40 m with a slope angle of 45° and a symmetrical shape. Calculate the cross-sectional area of the trapezoid for the open channel using Eq. (5):

$$A = \frac{0.85 + 0.40}{2} \times 0.40 = 0.25\, m^2$$

The calculated cross-sectional area of the irrigation channel was 0.25 m². The channel volume was determined by multiplying the calculated cross-sectional area by the channel length of 1.00 m, as expressed in Eq. (6).

$$V = A \times \ell$$

$$V = 0.25 \times 1.00 = 0.25\, m^3$$

The calculated water volume required to fill the 1-meter-long channel was 0.25 m³, equivalent to 250 liters. During the field test, the time required to fill the channel was recorded as 56.15 seconds. Based on the channel volume and the recorded filling time, the channel filling flow rate was calculated using Eq. (7), as follows:

$$Q_{\text{fill}} = \frac{V}{t} = \frac{A\ell}{t}$$

$$Q_{\text{fill}} = \frac{0.25 \times 1.00}{56.15}$$

$$Q_{\text{fill}} = 0.00445\, m^3/s = 267.17\, L/min$$

The channel filling flow rate was calculated as 0.00445 m³/s, equivalent to 267.17 L/min. This value is close to the pump discharge of 267.83 L/min reported at the preferred operating frequency of 40 Hz, with a difference of 0.66 L/min (0.25%). This comparison indicates reasonable agreement between the calculated pump discharge and the channel filling flow rate obtained from the field test.

Next, the water loss in the irrigation channel was assessed based on field data. The field test was conducted during the dry season, when the surrounding soil was dry and visibly cracked. The irrigation channel was initially empty, no water outflow occurred during the test, and rainfall and evaporation were considered negligible. Therefore, $V_{\text{out}} = 0$ and the change in water storage was determined from the final retained water volume. Based on field observations, the total incoming water volume was 0.65 m³, while the final retained water volume in the channel was 0.25 m³. Since the channel was initially empty, the change in water storage was:

$$\Delta V_{\text{storage}} = 0.25 - 0 = 0.25\ \text{m}^3$$

Substituting these values into Eq. (8), the estimated water loss was:

$$V_{\text{loss}} = 0.65 - 0 - 0.25 = 0.40\ \text{m}^3$$

To determine the percentage of water loss relative to the total water flow, Eq. (9) is used:

$$Loss(\%) = \left(\frac{0.40}{0.65}\right) \times 100 = 61.54\%$$

The 61.54% water loss indicates low distribution efficiency due to infiltration and seepage through the existing open soil channels. Although the pump discharges 270 L/min, only a limited portion of the water can be effectively distributed across the cultivated area. The low soil moisture content of

19.71% measured in the laboratory also contributes to water loss because the dry soil has a high infiltration capacity, particularly during the dry season. Therefore, improvements and conservation of the irrigation water distribution system are needed. Recent studies provide several potential alternatives. Zakir-Hassan et al. [34] reported that lining irrigation channels reduced seepage losses by 78% on average, with reductions ranging from 58% to 94%. In addition, Ashour et al. [35] reported that piped conveyance systems achieved up to 98% conveyance efficiency, corresponding to 2% conveyance loss. For field application, Reinders [36] reported 5% total system losses for surface and subsurface drip irrigation under their default design values. These findings indicate that replacing the existing open soil channel with a lined or closed conveyance system, combined with more efficient field application such as drip irrigation, could substantially reduce water losses in the present irrigation system.

Further analysis examined crop irrigation water requirements based on the total requirements of horticultural crops over an area of 2,500 m² (0.25 ha). The effective water requirement for horticultural crops such as chili, tomato, and mustard ranges from 5–6 mm/day. In this study, a conservative value of 5 mm/day or 5 liters/m²/day was used. Thus, the volume of water requirements can be calculated using Eq. (10):

$$Q_{plants} = 2{,}500\ m^2 \times 5\ L/m^2 = 12{,}500\ L/day = 12.5\ m^3/day$$

To effectively meet the plants' water requirements of 12.5 m³/day, the total volume of water that must be supplied by the irrigation system (Q_{total}) is calculated by taking into account a loss of 61.54% using Eq. (11):

$$Q_{total} = \frac{12.5}{1 - 0.6154} = \frac{12.5}{0.3846} = 32.5\ m^3/day$$

To meet the clean water requirements of the plants, which amount to 12.5 m³/day, the system must pump 32.5 m³/day due to distribution losses of more than 60%, meaning that only about 38% of the water is effectively utilized by the plants. This condition significantly affects energy efficiency and pump operating time. With an average pump flow rate of 4.5 L/s (270 L/minute), the daily operating time to meet the Q_{total} can be calculated using Eq. (12):

$$t = \frac{32{,}500}{270} = 120.37\ min\ \approx 2.006 \text{ hours}$$

$$\text{Approximately} = 120.37\ min\ \approx 2\ h\ 0\ min\ 22\ s$$

The submersible pump has a power rating of 750 W. The daily irrigation requirement (Q total) was previously calculated at 32.5 m³/day, and the pump can deliver a discharge of 4.5 L/s, or 270 L/minute. Therefore, the electrical energy required by the pump during 2 hours of operation is:

$$E_{pump} = 750w \times 2.006 \text{ hours} = 1{,}504.50\ Wh$$

With an energy requirement of 1,504.50 Wh/day and the solar panels generating 1,660.73 Wh/day after efficiency losses, there is still an energy surplus of 160.73 Wh/day. However, even though technically sufficient, the available energy margin is relatively small. In solar-based systems, energy availability depends heavily on weather conditions and daily solar radiation intensity. Decreased irradiation from cloud cover, rain, or seasonal changes can significantly reduce daily energy production, potentially leaving the system unable to meet full pump demand in a single day.

3.2 Socio-technical feasibility assessment

3.2.1 Social aspects

The socio-technical assessment involved 30 horticultural farmers. The interview results indicate a generally positive perception of the solar-powered irrigation system. 26 of 30 farmers (86.67%) expressed interest in adopting the technology because it could reduce dependence on conventional fuel and lower irrigation operating costs. Regarding system operation, 21 of 30 farmers (70.00%) found the system easy to operate, mainly because operation involved the control panel and VFD frequency setting. However, only 13 of 30 farmers (43.33%) reported being able to perform basic maintenance independently, such as checking electrical connections, cleaning solar panels, and inspecting system components.

These results indicate that technology acceptance among the participating farmers was relatively high, whereas technical self-reliance for maintenance was more limited. This finding is particularly relevant in remote agricultural areas where access to technical services and replacement components is limited.

3.2.2 Technical aspects

A socio-technical feasibility assessment evaluated the integration between the solar-powered submersible pump irrigation system's performance and farmers' socio-economic capacity to use and manage the technology. Field observations showed that the system operated optimally with a flow rate of 267–270 L/minute at a working frequency of 40 Hz. This flow rate met the daily irrigation needs of 2,500 m² of horticultural crops, which required 12.5 m³/day of water, with the system operating for 2 hours per day. The pump has a power of 750 W and a daily energy consumption of 1,504.50 Wh, which is still within the solar panel's daily production capacity of 1,660.73 Wh. These findings indicate that the sustainable irrigation system using a submersible pump for horticultural crops is technically feasible.

Quantitatively, the system's reliability can be measured by the ratio of the pump's energy requirement (E_p) to the energy available from the solar panels (E_s).

$$R = \frac{E_p}{E_s} = \frac{1{,}504.50}{1{,}660.73} = 0.90$$

With an R value < 1, the system remains safe, but because it is close to 1, it is vulnerable to energy fluctuations from weather or increased water demand. To strengthen sustainability, the water distribution system should be optimized, for example by providing water storage tanks as a reserve for irrigation.

3.2.3 Economic aspects

An economic analysis was conducted by comparing a solar-powered submersible pump irrigation system with a conventional irrigation system for a 0.25 ha horticultural field. The initial investment for the solar-powered system was IDR 55,000,000, while its routine maintenance cost was IDR

750,000 per year. The conventional irrigation cost, including pumping, operator, and maintenance expenses, was IDR 4,200,000 per cropping season. With four cropping seasons per year, the annual cost of the conventional system was calculated as follows:

$$C_{konvensional} = 4 \times IDR\ 4{,}200{,}000 = IDR\ 16{,}800{,}000/Year$$

The cost of the solar-powered system was calculated by accounting for routine maintenance and annualized operating and component-replacement costs. For the initial estimate, the $LiFePO_4$ battery replacement cost of IDR 15,000,000, with a service life of 10 years, resulted in an equivalent annual cost of IDR 1,500,000. The inverter replacement cost of IDR 5,000,000, with a service life of 10 years, resulted in an annual cost of IDR 500,000. Similarly, the VFD replacement cost of IDR 2,000,000 with a service life of 10 years resulted in an annual cost of IDR 200,000, while the pump replacement cost of IDR 5,000,000 with a service life of 5 years resulted in an annual cost of IDR 1,000,000. In addition, an annual allowance of IDR 1,470,690 was allocated for supplementary operating expenses and minor components, bringing the total equivalent annual cost, excluding routine maintenance, to IDR 4,670,690. Accordingly, the total annual cost of the solar-powered system was calculated by adding the routine maintenance cost to this amount.

$$\begin{aligned} C_{PV-system} &= IDR\ 750{,}000 + IDR\ 4{,}670{,}000 \\ &= IDR\ 5{,}420{,}690/Year \end{aligned}$$

The net annual savings were calculated as the difference between the annual costs of the conventional irrigation system and the solar-powered system, as follows:

$$\begin{aligned} C_{Savings} &= IDR\ 16{,}800{,}000 - IDR\ 5{,}420{,}690 \\ &= IDR\ 11{,}379{,}310/Year \end{aligned}$$

The payback period (PP) was then calculated by dividing the initial investment by the net annual savings. The resulting payback period was:

$$PP = \frac{IDR\ 55{,}000{,}000}{IDR\ 11{,}379{,}310} = 4.8333\ years \approx 5\ years$$

This calculation focuses on the overall investment payback without an in-depth micro-level economic analysis.

4. CONCLUSIONS

This study evaluates the initial technical, operational, social, and economic performance of a solar-powered submersible pump irrigation system for horticulture in a remote area of Merauke, Indonesia. A 900 Wp PV array generated an average of 1,962.11 Wh/day, ranging from 1,785.05 to 2,070.00 Wh/day over seven consecutive days during the dry season. Pump discharge was regulated using a VFD. The flow rate increased from 18.31 L/min at 21 Hz to 350.86 L/min at 50 Hz. Although the lowest SEC of 52.17 Wh/m³ was recorded at 50 Hz, an inverter overload alarm occurred at this frequency. Therefore, 40 Hz was considered a more suitable operating point under the tested conditions, delivering 267.83 L/min with an SEC of 63.09 Wh/m³. Energy balance analysis indicated an average inverter efficiency of 90.97%, a battery bidirectional efficiency of 95.00%, and a VFD efficiency of 97.94% at 40 Hz. The calculated combined efficiency was 84.64%, corresponding to cumulative conversion and storage losses of 15.36%. Based on this efficiency, the theoretically available energy was 1,660.73 Wh/day, and the pump consumed 1,504.5 Wh/day. These findings indicate that a sustainable irrigation system powered by solar energy is technically feasible.

Surface irrigation channel testing showed that only 0.25 m³ of the 0.65 m³ discharged was retained, resulting in 61.54% water losses, primarily due to infiltration and seepage. Meeting the effective irrigation requirement of 12.5 m³/day for 2,500 m² of horticultural land would require a supply of 32.5 m³/day. Lined channels, closed-pipe distribution, and efficient irrigation methods could help reduce these losses. Of 30 farmers, 86.67% expressed interest in adopting the system, 70.00% considered it easy to operate, and 43.33% reported maintenance difficulties. With an initial investment of IDR 55,000,000 and annual savings of IDR 11,379,310, the reported payback period was five years. These findings demonstrate the feasibility of solar-powered horticultural irrigation systems in remote areas of the region. However, they do not yet indicate the potential for large-scale implementation. Further testing at various locations and over a longer evaluation period is needed to validate their performance and enable broader implementation.

REFERENCES

[1] Mekouar, M.A. (2023). Food and Agriculture Organization of the United Nations (FAO). Yearbook of International Environmental Law, 34(1): yvae031. https://doi.org/10.1093/yiel/yvae031

[2] IPCC. (2022). Climate Change 2022: Mitigation of Climate Change. Contribution of Working Group III to the Sixth Assessment Report of the Intergovernmental Panel on Climate Change. Cambridge University Press. https://doi.org/10.1017/9781009157926

[3] Thawley, C., Crystallin, M., Verico, K. (2024). Towards a higher growth path for Indonesia. Bulletin of Indonesian Economic Studies, 60(3): 247-282. https://doi.org/10.1080/00074918.2024.2432035

[4] Ambarwati, A., Chazali, C., Sadoko, I., White, B. (2024). Youth and agriculture in Indonesia. In Becoming a Young Farmer: Young People's Pathways into Farming: Canada, China, India and Indonesia. Palgrave Macmillan, Cham, pp. 303-335. https://doi.org/10.1007/978-3-031-15233-7_11

[5] Wibowo, D.P., Al Vayed, D., Mardiatmi, B.D. (2024). Strengthening local food security for climate change adaptation: Lessons from Merauke-Papua Indonesia. In Climate Crisis, Social Responses and Sustainability: Socio-ecological Study on Global Perspectives. Cham: Springer Nature Switzerland, pp. 645-664. https://doi.org/10.1007/978-3-031-58261-5_28

[6] Hariyanto, Rusdi, M., Jayadi. (2023). Implementation of solar-powered submersible pump technology (PSTSP) to increase rainfed rice field production. Engagement, 7(1): 200-210. https://doi.org/10.29062/engagement.v7i1.1096

[7] Yahaya, A.A., Hassan, S.A., Usman, A.M., Mohammed, I., Yisa, E. (2025). Development of a mathematical model to analyze the impact of fuel subsidy on rice

production in Niger State, Nigeria. International Journal of Research and Innovation in Applied Science, 10(1): 145-151. https://doi.org/10.51584/ijrias.2025.1001012

[8] Patel, P.M., Scott, C.A., Brent, D.A. (2025). Four birds with one stone? Opportunities and challenges in adopting solar irrigation for a sustainable water-energy-food nexus with carbon credits. Water International, 50(3-4): 235-258. https://doi.org/10.1080/02508060.2024.2345494

[9] Batoukhteh, F., Darzi-Naftchali, A., Motevali, A., Karandish, F., Berger, M. (2025). Evaluating the sustainability of wheat irrigation systems: Using life cycle assessment to monitor the water-energy-food-environment nexus. Agricultural Water Management, 315: 109521. https://doi.org/10.1016/j.agwat.2025.109521

[10] Pamuttu, D.L., Akbar, M., Andika, A.P., Hariyanto, H. (2023). An investigation of hybrid renewable energy potential by harnessing traffic flow. International Journal of Heat and Technology, 41(1): 239-246. https://doi.org/10.18280/ijht.410126

[11] Hariyanto, H., Parenden, D., Vincēviča-Gaile, Z., Gamawati Adinurani, P. (2020). Potential of new and renewable energy in Merauke Regency as the future energy. E3S Web of Conferences, 190: 00012. https://doi.org/10.1051/e3sconf/202019000012

[12] Al-Zubaidi, E.D.A., Ismael, H.A.A., Abdulrahman, M.M., et al. (2024). Revolutionizing urban water management: A green-aware study based on innovative approach. International Journal of Sustainable Development and Planning, 19(12): 4563-4572. https://doi.org/10.18280/ijsdp.191205

[13] Kurpaska, S., Knaga, J., Latała, H., Cupiał, M., Konopacki, P., Hołownicki, R. (2020). The comparison of different types of heat accumulators and benefits of their use in horticulture. Sensors, 20(5): 1417. https://doi.org/10.3390/s20051417

[14] Mahmudul Haque, A.K.M., Akram Ullah, S.M., Sikdar, M.M., et al. (2022). Integrating environmental governance into sustainable urban development in Bangladesh. International Journal of Sustainable Development and Planning, 17(5): 1471-1478. https://doi.org/10.18280/ijsdp.170511

[15] Sundaram, M., Chelladurai, J., Anand, M., Varunraj, P., Sharma, S., El Haj Assad, M. (2022). Performance evaluation of energy-efficient submersible tubular brushless permanent magnet motor for irrigation application. Arabian Journal for Science and Engineering, 47(11): 14327-14341. https://doi.org/10.1007/s13369-022-06744-2

[16] Yang, Y., Wang, H., Wang, C., et al. (2024). An entropy efficiency model and its application to energy performance analysis of a multi-stage electric submersible pump. Energy, 288: 129741. https://doi.org/10.1016/j.energy.2023.129741

[17] Abdelhamid, M.A., Abdelkader, T.K., Sayed, H.A.A., Zhang, Z., Zhao, X., Atia, M.F. (2025). Design and evaluation of a solar powered smart irrigation system for sustainable urban agriculture. Scientific Reports, 15(1): 11761. https://doi.org/10.1038/s41598-025-94251-3

[18] Kok, C.L., Ho, C.K., Koh, Y.Y., Tay, W.X., Teo, T.H. (2024). Innovative energy sustainable solutions for urban infrastructure: Implementing micro-pumped hydro storage in Singapore's multi-level carparks. Applied Sciences, 14(17): 7531. https://doi.org/10.3390/app14177531

[19] Abhilash, P., Kumar, R.N., Kumar, R.P. (2021). Solar powered water pump with single axis tracking system for irrigation purpose. Materials Today: Proceedings, 39: 553-557. https://doi.org/10.1016/j.matpr.2020.08.336

[20] Ouedraogo, K.R., Tete, K.H.S., Soro, Y.M., Darga, A. (2025). Solar water pumping systems for a sustainable development of the market gardening sector in Burkina Faso. Discover Sustainability, 6(1): 969. https://doi.org/10.1007/s43621-025-01636-5

[21] Dimara, P.A., Purwanto, R.H., Sunarta, S., Wardhana, W. (2021). The spatial distribution of sago palm landscape Sentani watershed in Jayapura District, Papua Province, Indonesia. Biodiversitas Journal of Biological Diversity, 22(9): 3811-3820. https://doi.org/10.13057/biodiv/d220926

[22] Karnib, A., Elbendary, N., Abouelhassan, W., Dawoud, M. (2025). Sustainability assessment of solar-powered drip irrigation for sugarcane in Egypt: A water–energy–food–ecosystem nexus perspective. World Water Policy, 11(2): 393-409. https://doi.org/10.1002/wwp2.12247

[23] Maka, A.O.M., Chaudhary, T.N. (2024). Performance investigation of solar photovoltaic systems integrated with battery energy storage. Journal of Energy Storage, 84: 110784. https://doi.org/10.1016/j.est.2024.110784

[24] Oyeshile, O., Fadare, D.A., Kazeem, R.A., et al. (2023). Development of a low-cost and modular vertical farming rig for sustainable farming process. Instrumentation Mesure Métrologie, 22(3): 95-104. https://doi.org/10.18280/i2m.220302

[25] Li, Z., Yang, T., Zhang, J., et al. (2024). New paradigms of water-enabled electrical energy generation. SusMat, 4(3): e206. https://doi.org/10.1002/sus2.206

[26] Wang, M., Zhang, L., Hu, X., Zhao, J., Chao, X., Fang, X. (2024). Investigation of flow field characteristics in hose pumps under various operating conditions and their impact on gap leakage. Physics of Fluids, 36(1): 014130. https://doi.org/10.1063/5.0187877

[27] Wu, Q., Xu, B., Liu, X., et al. (2024). Modeling and optimization for submersible pump tubular linear motor based on dynamic load analysis. IEEE Access, 12: 177160-177172. https://doi.org/10.1109/ACCESS.2024.3485084

[28] Fan, Y., Chen, H., Gao, Z., et al. (2023). Water distribution and scheduling model of an irrigation canal system. Computers and Electronics in Agriculture, 209: 107866. https://doi.org/10.1016/j.compag.2023.107866

[29] Yan, W., Li, F., Zhao, Y. (2022). Determination of irrigation water quantity and its impact on crop yield and groundwater. Agricultural Water Management, 273: 107900. https://doi.org/10.1016/j.agwat.2022.107900

[30] El-Molla, D.A., El-Molla, M.A. (2021). Seepage losses from trapezoidal earth canals with an impervious layer under the bed. Water Practice & Technology, 16(2): 530-540. https://doi.org/10.2166/wpt.2021.010

[31] Liu, J., Sun, B., Shen, H., et al. (2022). Crop water requirement and utilization efficiency-based planting structure optimization in the Southern Huang-Huai-Hai Plain. Agronomy, 12(9): 2219. https://doi.org/10.3390/agronomy12092219

[32] Bhavsar, D., Limbasia, B., Mori, Y., Aglodiya, M.I., Shah, M. (2023). A comprehensive and systematic study in smart drip and sprinkler irrigation systems. Smart Agricultural Technology, 5: 100303.

https://doi.org/10.1016/j.atech.2023.100303
[33] Phiri, E., Rowley, P.N., Blanchard, R.E. (2023). Addressing challenges in delivering sustainable rural water provision using solar water pumping in Malawi: A stakeholder analysis. Energies, 16(23): 7758. https://doi.org/10.3390/en16237758
[34] Zakir-Hassan, G., Kahlown, M.A., Punthakey, J.F., et al. (2023). Evaluation of hydraulic efficiency of lined irrigation channels – A case study from Punjab, Pakistan. Hydrology Research, 54(4): 523-546. https://doi.org/10.2166/nh.2023.105
[35] Ashour, M.A., Abdel Nasser, M.S., Abu-Zaid, T.S. (2024). Evaluation of the effects of improving tertiary earthen canals on water savings, conveyance efficiency, and agricultural productivity. Ain Shams Engineering Journal, 15(8): 102850. https://doi.org/10.1016/j.asej.2024.102850
[36] Reinders, F.B. (2022). Irrigation water use efficiency: A water balance approach. River, 1(2): 142-148. https://doi.org/10.1002/rvr2.18